5
In Situ Adaptive Tabulation

In this chapter is described the *in situ adaptive tabulation* (ISAT) technique proposed by Pope (1997) [70] that is used to reduce the computational cost associated to the solution of Eq.(4.2).

5.1
Linearized Reaction Mapping

Consider a composition $\boldsymbol{\phi}$[1] and an *initial composition* $\boldsymbol{\phi}_0$, so that the series expansion of the reaction mapping of the composition around the initial one is

$$\boldsymbol{R}(\boldsymbol{\phi}, t) = \boldsymbol{R}(\boldsymbol{\phi}_0, t) + \boldsymbol{A}(\boldsymbol{\phi}_0, t)\delta\boldsymbol{\phi} + \mathcal{O}(||\delta\boldsymbol{\phi}||_2^2), \tag{5.1}$$

where the *composition displacement* is given by

$$\delta\boldsymbol{\phi} \equiv \boldsymbol{\phi} - \boldsymbol{\phi}_0, \tag{5.2}$$

the *mapping gradient matrix* is the $n_\phi \times n_\phi$ matrix $\boldsymbol{A}(\boldsymbol{\phi}_0, t)$ which is represented in the canonical base by the components

$$A_{ij}(\boldsymbol{\phi}_0, t) \equiv \frac{\partial R_i}{\partial \phi_{0_j}}(\boldsymbol{\phi}_0, t), \tag{5.3}$$

and $\mathcal{O}(||\delta\boldsymbol{\phi}||_2^2)$ denotes terms that have order $||\delta\boldsymbol{\phi}||_2^2$, where the Euclidean norm of a vector $\boldsymbol{\psi}$, denoted by $||\cdot||_2$, is given by the expression

$$||\boldsymbol{\psi}||_2 \equiv \sqrt{\sum_{i=1}^{n_\phi} \psi_i^2}. \tag{5.4}$$

The *linear approximation*

$$\boldsymbol{R}^l(\boldsymbol{\phi}, t) \equiv \boldsymbol{R}(\boldsymbol{\phi}_0, t) + \boldsymbol{A}(\boldsymbol{\phi}_0, t)\delta\boldsymbol{\phi}, \tag{5.5}$$

is second order accurate at a connected region of composition space centered at $\boldsymbol{\phi}_0$. The shape of this region is unknown before the calculations, but the ISAT technique approximates this region by a hyper-ellipsoid, as will be shown in section 5.2.

[1] In this chapter the superscript $^{(j)}$ is omitted for the sake of notation simplicity.

The *local error* of the linear approximation is defined as the Euclidean norm of the difference between the reaction mapping at $\boldsymbol{\phi}$ and the linear approximation for it around $\boldsymbol{\phi}_0$

$$\varepsilon \equiv ||\boldsymbol{R}(\boldsymbol{\phi}, t) - \boldsymbol{R}^l(\boldsymbol{\phi}, t)||_2. \tag{5.6}$$

5.2 Ellipsoid of Accuracy

The accuracy of the linear approximation at $\boldsymbol{\phi}_0$ is controlled only if the local error is smaller than a positive *error tolerance* ε_{tol}, which is heuristically chosen. The *region of accuracy* is defined as the connected region of composition space centered at $\boldsymbol{\phi}_0$ where local error is not greater than ε_{tol}.

For instance, assume a *constant approximation* for the reaction mapping at $\boldsymbol{\phi}$, i.e., $\boldsymbol{R}^c(\boldsymbol{\phi}, t) \equiv \boldsymbol{R}(\boldsymbol{\phi}_0, t)$, instead of the linear approximation defined in Eq.(5.5). The local error to leading order is

$$\varepsilon = ||\boldsymbol{A}\delta\boldsymbol{\phi}||_2, \tag{5.7}$$

and thus the region of accuracy ($\varepsilon \leq \varepsilon_{tol}$) is

$$\delta\boldsymbol{\phi}^{\mathrm{T}}\boldsymbol{A}^{\mathrm{T}}\boldsymbol{A}\delta\boldsymbol{\phi} \leq \varepsilon_{tol}^2. \tag{5.8}$$

The *singular value decomposition* (SVD) states that the reaction gradient matrix has a factorization in the form

$$\boldsymbol{A} = \boldsymbol{U}\boldsymbol{\Sigma}\boldsymbol{V}^{\mathrm{T}}, \tag{5.9}$$

where $\boldsymbol{U}$ and $\boldsymbol{V}$ are real square orthogonal matrices and $\boldsymbol{\Sigma}$ is a real square diagonal matrix with nonnegative elements on the diagonal (Golub & Van Loan, 1996) [22]. A real square matrix $\boldsymbol{V}$ is orthogonal if, and only if, its transpose is equal to its inverse, i.e., $\boldsymbol{V}^{\mathrm{T}} = \boldsymbol{V}^{-1}$. Therefore, Eq.(5.8) reads

$$\delta\boldsymbol{\phi}^{\mathrm{T}}\boldsymbol{V}\boldsymbol{\Sigma}^{\mathrm{T}}\boldsymbol{\Sigma}\boldsymbol{V}^{\mathrm{T}}\delta\boldsymbol{\phi} \leq \varepsilon_{tol}^2, \tag{5.10}$$

which is a hyper dimensional quadratic form centered at $\boldsymbol{\phi}_0$.

The matrix $\boldsymbol{\Sigma}^{\mathrm{T}}\boldsymbol{\Sigma} = \boldsymbol{\Sigma}^2$ is diagonal, so its eigenvalues are σ_i^2 ($i = 1, \cdots, n_\phi$) where the σ_i are the singular values of $\boldsymbol{A}$. Since all the eigenvalues of $\boldsymbol{\Sigma}^2$ are nonnegative, i.e., $\sigma_i^2 \geq 0$, the quadratic form above has the shape of a hyper-ellipsoid centered at $\boldsymbol{\phi}_0$, which is dubbed *ellipsoid of accuracy* (EOA). A sketch of the region of accuracy for a constant approximation is shown in Figure 5.1.

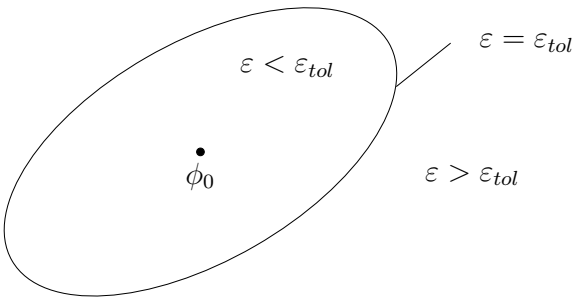

Figure 5.1: The region of accuracy for a constant approximation is a hyper-ellipsoid in composition space.

Therefore, the EOA is characterized by the center, $\boldsymbol{\phi}_0$, the orthogonal matrix $\boldsymbol{V}$ the diagonal matrix $\boldsymbol{\Sigma}$ and the error tolerance ε_{tol}. In fact, the columns of the matrix $\boldsymbol{V}$ define the EOA principal directions and the half-length of the EOA in each principal direction is given by

$$l_i \equiv \frac{\varepsilon_{tol}}{\sigma_i}. \tag{5.11}$$

In cases when $\sigma_i \to 0^+$ or $\sigma_i \to \infty$, the hyper-ellipsoid degenerates. To avoid the situation where the region of accuracy is a degenerate hyper-ellipsoid, a modified version of the reaction gradient matrix, $\widetilde{\boldsymbol{A}}$, is considered

$$\widetilde{\boldsymbol{A}} \equiv \boldsymbol{U}\widetilde{\boldsymbol{\Sigma}}\boldsymbol{V}^{\mathrm{T}}, \tag{5.12}$$

where $\widetilde{\boldsymbol{\Sigma}}$ is a diagonal matrix with elements given by

$$\widetilde{\sigma}_i \equiv \min\left(\frac{\varepsilon_{tol}}{\kappa u_r}, \widetilde{\widetilde{\sigma}}_i\right), \tag{5.13}$$

where u_r is the *machine unit roundoff*[2], the lower bound κ is a positive real number such that $\kappa u_r < 2\varepsilon_{tol}$ and

$$\widetilde{\widetilde{\sigma}}_i \equiv \max\left(1/2, \sigma_i\right). \tag{5.14}$$

This modification ensures that the modified half-length of EOA, $\widetilde{l}_i$, is bounded

$$\kappa u_r \leq \widetilde{l}_i \leq 2\varepsilon_{tol}. \tag{5.15}$$

Also, the restriction imposed by Eq.(5.15) in EOA half-length defines a *band-pass filter*[3] for chemical time scales, since the i-th singular value of reaction gradient matrix is related to i-th chemical species frequency through the rate of reaction of this species.

[2]The machine unit roundoff, u_r, is defined as the smallest floating point number such that `1.0` $+ u_r >$ `1.0`. Using double precision in a 32 bits digital computer, a typical value for u_r is 10^{-16}.

[3]A band-pass filter allows the passage of frequencies within a certain range and attenuates frequencies outside of this range.

It is noteworthy that the modification to avoid small singular values, Eq.(5.14), was proposed in the original work of Pope (1997) [70], whereas the change to avoid large singular values, Eq.(5.13), is a original contribution of the present work.

The product of the modified reaction gradient matrix transposed by itself is a symmetric positive defined matrix, and has a *Cholesky decomposition* of the form

$$\widetilde{\boldsymbol{A}}^{\mathrm{T}}\widetilde{\boldsymbol{A}} = \boldsymbol{L}\boldsymbol{L}^{\mathrm{T}}, \tag{5.16}$$

where $\boldsymbol{L}$ is lower triangular matrix, (Golub & Van Loan, 1996) [22]. Thus, another natural way of describing the EOA is

$$\delta\boldsymbol{\phi}^{\mathrm{T}}\boldsymbol{L}\boldsymbol{L}^{\mathrm{T}}\delta\boldsymbol{\phi} \leq \varepsilon_{tol}^2. \tag{5.17}$$

Note that this decomposition is computed after performing the SVD given in Eq.(5.9) and recomposing $\widetilde{\boldsymbol{A}}$ using Eq.(5.16).

The cost of the EOA representation, in terms of computer memory, involves storing three elements, the vector $\boldsymbol{\phi}_0$ and the matrices $\boldsymbol{V}$ and $\widetilde{\boldsymbol{\Sigma}}$, which requirements, respectively, scale as n_ϕ, n_ϕ^2 and n_ϕ ($\widetilde{\boldsymbol{\Sigma}}$ is diagonal) floating point numbers. So, the total memory cost is $n_\phi^2 + 2n_\phi$.

On the other hand, the Cholesky representation, Eq.(5.17), stores only two elements, the vector $\boldsymbol{\phi}_0$ and the matrix $\boldsymbol{L}$. Each one, respectively, needing to store n_ϕ and $\frac{n_\phi(n_\phi+1)}{2}$ ($\boldsymbol{L}$ is lower triangular) floating point numbers. So, the total memory cost is $\frac{1}{2}n_\phi^2 + \frac{3}{2}n_\phi$.

Both representations of the EOA are $\mathcal{O}(n_\phi^2)$, but using the Cholesky approach it is possible to save in memory storage $\frac{1}{2}n_\phi^2 + \frac{1}{2}n_\phi$ floating point positions. Thus the Cholesky representation is used in this work.

5.3 Hyper-ellipsoid Growth

In this section is discussed a geometric problem related to the adaptive step of ISAT technique. Consider the original hyper-ellipsoid centered at $\boldsymbol{\phi}_0$ and a *query composition*, $\boldsymbol{\phi}_q$, outside it, Figure 5.2. The problem is to determine a new hyper-ellipsoid of minimum hyper-volume, centered at $\boldsymbol{\phi}_0$, which encloses both the original hyper-ellipsoid and the point $\boldsymbol{\phi}_q$. A strategy to allow the growth of the hyper-ellipsoid proposed by Pope (2008) [71] is presented below.

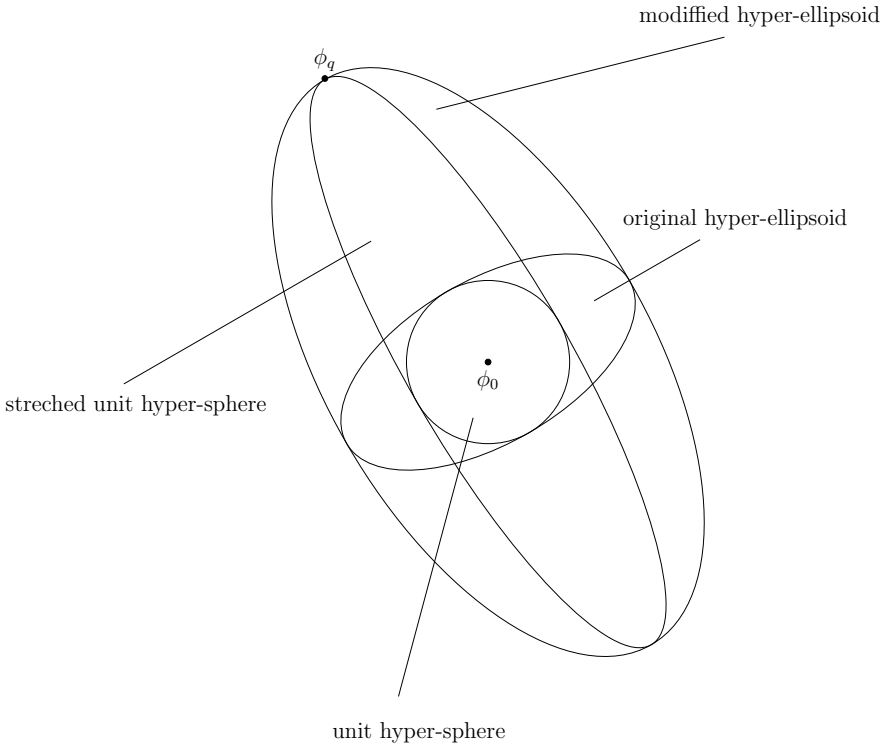

Figure 5.2: Growth process of the original hyper-ellipsoid.

Consider the affine transformation that maps a composition $\boldsymbol{\phi}$ in $\mathcal{C}$ into a transformed composition

$$\widetilde{\boldsymbol{\phi}} \equiv \frac{1}{\varepsilon_{tol}} \boldsymbol{L}^{\mathrm{T}} \delta\boldsymbol{\phi}. \tag{5.18}$$

It is obvious that $\widetilde{\boldsymbol{\phi}}$ also is in $\mathcal{C}$ (see section 3.6.1) and, for any $\boldsymbol{\phi}$ in the original hyper-ellipsoid, it is possible to see, with the help of Eq.(5.17), that

$$||\widetilde{\boldsymbol{\phi}}||_2^2 = \widetilde{\boldsymbol{\phi}}^{\mathrm{T}} \widetilde{\boldsymbol{\phi}} = \frac{1}{\varepsilon_{tol}^2} \delta\boldsymbol{\phi}^{\mathrm{T}} \boldsymbol{L}\boldsymbol{L}^{\mathrm{T}} \delta\boldsymbol{\phi} \leq 1, \tag{5.19}$$

which is equivalent to

$$\widetilde{\phi}_1^2 + \cdots + \widetilde{\phi}_{n_\phi}^2 \leq 1. \tag{5.20}$$

Therefore, it is possible to conclude that the transformation defined by Eq.(5.18) maps the original hyper-ellipsoid into the unit hyper-sphere in $\mathcal{C}$, as sketched in Figure 5.2. Likewise, applying this affine transformation to the query composition outside the EOA, $\boldsymbol{\phi}_q$, the modified query composition is obtained

$$\widetilde{\boldsymbol{\phi}}_q = \frac{1}{\varepsilon_{tol}} \boldsymbol{L}^{\mathrm{T}} \delta\boldsymbol{\phi}_q. \tag{5.21}$$

Now consider the linear transformation that stretches the unit hyper-sphere in $\mathcal{C}$ in the direction of the vector $\widetilde{\boldsymbol{\phi}}_q$, as sketched in Figure 5.2.

This transformation is performed by the rank-one modification defined as

$$\boldsymbol{G} \equiv \boldsymbol{I} + \gamma \widetilde{\boldsymbol{\phi}}_q \widetilde{\boldsymbol{\phi}}_q^{\mathrm{T}}, \tag{5.22}$$

where $\boldsymbol{I}$ is the identity matrix and the constant γ, which is determined by the condition

$$\widetilde{\boldsymbol{\phi}}_q^{\mathrm{T}} \boldsymbol{G}\boldsymbol{G}^{\mathrm{T}} \widetilde{\boldsymbol{\phi}}_q = 1, \tag{5.23}$$

is given by

$$\gamma \equiv \left(\widetilde{\phi}_q^{-1} - 1\right) \widetilde{\phi}_q^{-2}, \tag{5.24}$$

being $\widetilde{\phi}_q = ||\widetilde{\boldsymbol{\phi}}_q||_2$.

To prove the last statement, suppose without loss of generality that the vector $\widetilde{\boldsymbol{\phi}}_q$ is aligned with the first vector of an orthonormal basis $\{\widehat{\boldsymbol{e}}_1, \cdots, \widehat{\boldsymbol{e}}_{n_\phi}\}$ in $\mathcal{C}$, i.e., $\widetilde{\boldsymbol{\phi}}_q = \widetilde{\phi}_q \widehat{\boldsymbol{e}}_1$. Thus,

$$\widehat{\boldsymbol{\phi}} \equiv \boldsymbol{G}^{\mathrm{T}} \widetilde{\boldsymbol{\phi}}, \tag{5.25}$$

reads as

$$\widehat{\boldsymbol{\phi}} = \widetilde{\boldsymbol{\phi}} + \left(\widetilde{\phi}_q^{-1} - 1\right) \widetilde{\phi}_1 \widehat{\boldsymbol{e}}_1, \tag{5.26}$$

which implies

$$\widehat{\phi}_1 = \frac{\widetilde{\phi}_1}{\widetilde{\phi}_q} \qquad \text{and} \qquad \widehat{\phi}_i = \widetilde{\phi}_i \qquad i = 2, \cdots, n_\phi. \tag{5.27}$$

Thus, it is possible to see that

$$\begin{aligned} ||\widehat{\boldsymbol{\phi}}||_2^2 &= \widehat{\phi}_1^2 + \cdots + \widehat{\phi}_{n_\phi}^2 && (5.28)\\ &= \frac{\widetilde{\phi}_1^2}{\widetilde{\phi}_q^2} + \widetilde{\phi}_2^2 + \cdots + \widetilde{\phi}_{n_\phi}^2 && (5.29)\\ &\leq \widetilde{\phi}_1^2 + \widetilde{\phi}_2^2 + \cdots + \widetilde{\phi}_{n_\phi}^2 && (5.30)\\ &\leq 1, && (5.31) \end{aligned}$$

or

$$\frac{\widetilde{\phi}_1^2}{\widetilde{\phi}_q^2} + \widetilde{\phi}_2^2 + \cdots + \widetilde{\phi}_{n_\phi}^2 \leq 1, \tag{5.32}$$

which is a hyper-ellipsoid with semi-axis equal to the unit in all directions except the first where it is equal to $\widetilde{\phi}_q$.

Returning to the original coordinate system, the modified hyper-ellipsoid equation, Figure 5.2, is given

$$\delta\boldsymbol{\phi}^{\mathrm{T}}\boldsymbol{L}\boldsymbol{G}\boldsymbol{G}^{\mathrm{T}}\boldsymbol{L}^{\mathrm{T}}\delta\boldsymbol{\phi} \leq \varepsilon_{tol}^2, \tag{5.33}$$

and the new Cholesky matrix, $\boldsymbol{L'}$, can be obtained from

$$\boldsymbol{L'}\boldsymbol{L'}^{\mathrm{T}} = (\boldsymbol{L}\boldsymbol{G})(\boldsymbol{L}\boldsymbol{G})^{\mathrm{T}}. \tag{5.34}$$

5.4 Adaptive Tabulation Procedure

As illustraded in Figure 3.1, the accessed region in composition space is much smaller than the realizable region, since it consists of the union of a finite number of composition trajectories along the realizable region. Therefore, the adaptive tabulation method needs to treat the accessed region only, whose shape is unknown prior to the integration of the system of equations given by Eq.(3.52).

Initially the ISAT algorithm receives the time step Δt and the tolerance ε_{tol}. Then, in every time step, the ISAT algorithm receives a query composition $\boldsymbol{\phi}_q$ and returns an approximation for the corresponding reaction mapping $\boldsymbol{R}(\boldsymbol{\phi}_q, t)$. This approximation is obtained via numerical integration of Eq.(4.2) or by the linear approximation $\boldsymbol{R}^l(\boldsymbol{\phi}_q, t)$.

During the chemically reactive flow calculation, some of the computed values are sequentially stored in a table for future use. This process is known as *in situ* tabulation.

In fact, the ISAT table created by the tabulation process includes the initial composition $\boldsymbol{\phi}_0$, the reaction mapping $\boldsymbol{R}(\boldsymbol{\phi}_0, t)$ and the mapping gradient matrix $\boldsymbol{A}(\boldsymbol{\phi}_0, t)$. Using these elements it is possible to construct the linear approximation, Eq.(5.5).

As the calculation proceeds, new query composition, $\boldsymbol{\phi}_q$, are received by ISAT, the table is transversed until finds a $\boldsymbol{\phi}_0$ that is a composition "close" to $\boldsymbol{\phi}_q$. Depending on the accuracy, the linear approximation around $\boldsymbol{\phi}_0$ is returned or the reaction mapping of $\boldsymbol{\phi}_q$ is obtained by direct integration of Eq.(4.2).

The ISAT table is a binary search tree, Figure 5.3, since this data structure allows searching for an information with a linear dependency on the complexity in the tree height. So, if the binary search tree is balanced, such as the one illustrated in Figure 5.3(a), the search complexity is only $\mathcal{O}(\log_2 n_{tab})$, where n_{tab} is the total number entries in the tree. A sequential search for the same information in a vector data structure costs $\mathcal{O}(n_{tab})$. Search for an information in a binary search tree that is not balanced, such as the one

shown in Figure 5.3(b), has the same cost as a sequential search in a vector. If $n_{tab} \gg 1$ than $\log_2 n_{tab} \ll n_{tab}$, justifying the option for the binary search tree as the storing table. For a deeper insight in tree data structures and searching algorithms see Knuth (1997) [38] and Knuth (1998) [39].

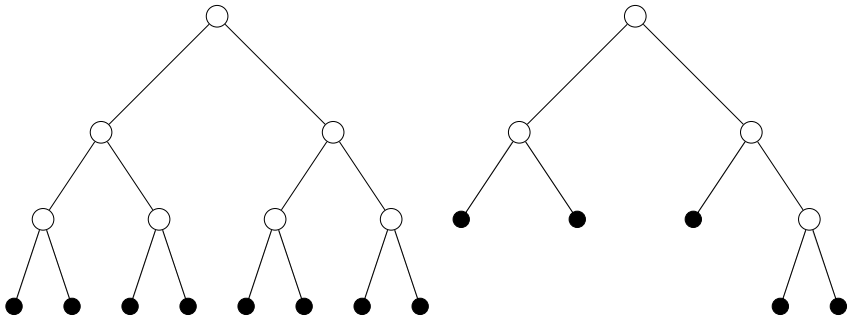

5.3(a): balanced tree 5.3(b): unbalanced tree

Figure 5.3: Sketch of the binary search trees created by ISAT algorithm (leaves are black and nodes white).

The binary search tree is basically formed by two types of elements, nodes and leaves. Each leaf of the tree stores the following data:

- $\boldsymbol{\phi}_0$: initial composition;
- $\boldsymbol{R}(\boldsymbol{\phi}_0, t)$: reaction mapping at $\boldsymbol{\phi}_0$;
- $\boldsymbol{A}(\boldsymbol{\phi}_0, t)$: mapping gradient matrix at $\boldsymbol{\phi}_0$;
- $\boldsymbol{L}$: EOA Cholesky matrix.

Each node of the binary search tree has an associated *cutting plane*. This plane is defined by a *normal vector*

$$\boldsymbol{v} \equiv \boldsymbol{\phi}_q - \boldsymbol{\phi}_0, \tag{5.35}$$

and a scalar

$$a \equiv \boldsymbol{v}^{\mathrm{T}} \left(\frac{\boldsymbol{\phi}_q + \boldsymbol{\phi}_0}{2} \right), \tag{5.36}$$

such that all composition $\boldsymbol{\phi}$ with $\boldsymbol{v}^T \boldsymbol{\phi} > a$ is deemed to be on the right of the cutting plane, all other compositions are on the left as sketched in Figure 5.4. The cutting plane construction defines a search criterion in the binary search tree.

If, during the calculation, a query point $\boldsymbol{\phi}_q$ is encountered that is within the region of accuracy, (i.e. $\varepsilon \leq \varepsilon_{tol}$), but outside the estimate of EOA, then the EOA growth proceeds as detailed in section 5.3.

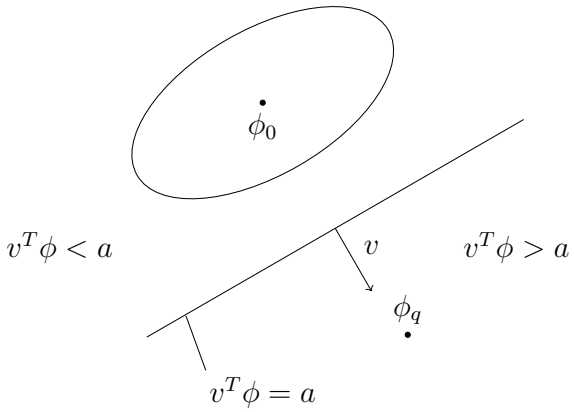

Figure 5.4: Sketch of cutting plane in relation to EOA position.

The first three items stored in the binary search tree leaf ($\boldsymbol{\phi}_0$, $\boldsymbol{R}(\boldsymbol{\phi}_0, t)$ *and* $\boldsymbol{A}(\boldsymbol{\phi}_0, t)$) are computed once, whereas $\boldsymbol{L}$ changes whenever the EOA is grown.

Once a query composition $\boldsymbol{\phi}_q$ is received by ISAT table, the binary search tree is initialized as a single leaf ($\boldsymbol{\phi}_0 = \boldsymbol{\phi}_q$) and the exact value of the reaction mapping is returned.

The following steps are:

1. Given a query composition the tree is transversed until a leaf ($\boldsymbol{\phi}_0$) is found.
2. Equation (5.17) is used to determinate if $\boldsymbol{\phi}_q$ is inside EOA or not.
3. If $\boldsymbol{\phi}_q$ is inside EOA, the reaction mapping is given by the linear approximation, Eq.(5.5). This is the first of three outcomes, called *retrieve*.
4. If $\boldsymbol{\phi}_q$ is outside EOA, direct integration is used to compute the reaction mapping, and the local error is measured by Eq.(5.6).
5. If the local error is smaller than tolerance, ε_{tol}, the EOA is grown according to the procedure presented in subsection 5.3 and the reaction mapping is returned. This outcome is called *growth*.
6. If local error is greater than the tolerance ε_{tol} and the maximum number of entries in the binary search tree is not reached, a new record is stored in the binary search tree based on $\boldsymbol{\phi}_q$ and the reaction mapping is returned. The original leaf is replaced by a node with the left leaf representing the old composition $\boldsymbol{\phi}_0$ and the right leaf the new one $\boldsymbol{\phi}_q$ as shown in Figure 5.5. This outcome is an *addition*.

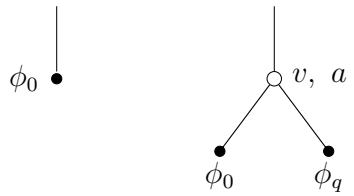

Figure 5.5: Binary search tree before and after the addition of a new node.

7. If the local error is greater than the tolerance ε_{tol} and the maximum number of entries in the binary search tree is reacted, the reaction mapping is returned. This outcome is called *direct evaluation*.

A flowchart showing all steps of ISAT algorithm is presented in Figure 5.6.

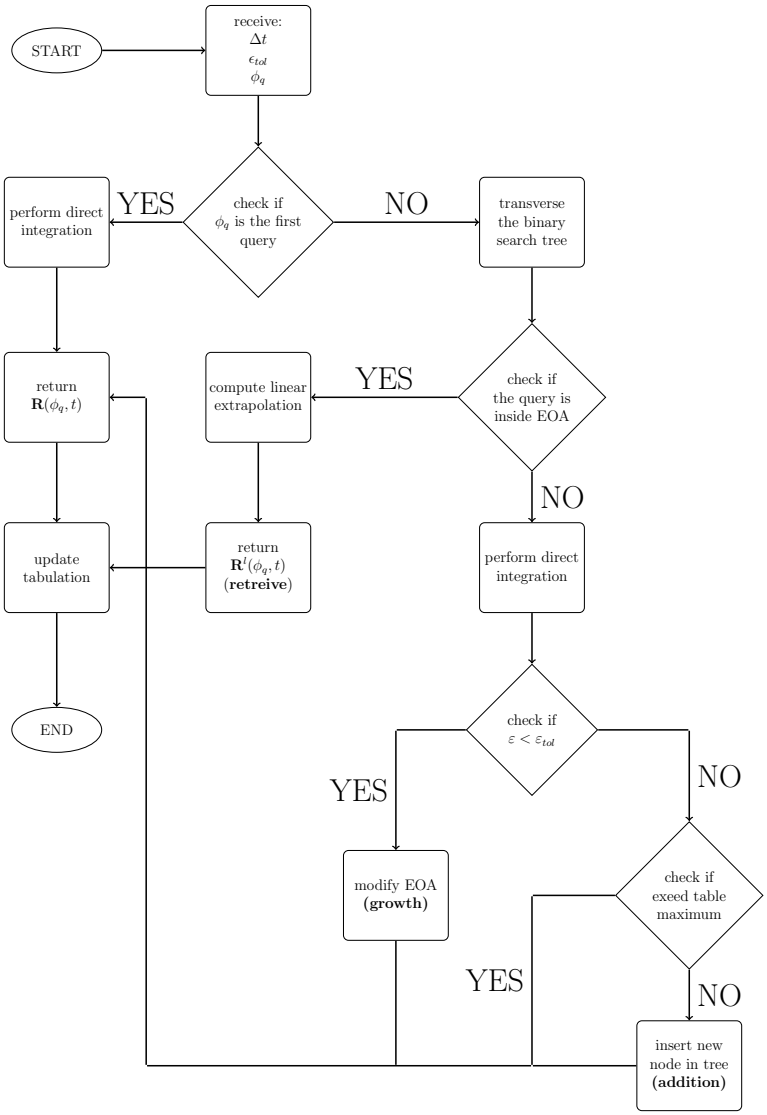

Figure 5.6: A flowchart showing all step of ISAT algorithm.